Development 136, 1791-1800 (2009) doi:10.1242/dev.032235

The tetraspanin Tm4sf3 is localized to the ventral pancreas and regulates fusion of the dorsal and ventral pancreatic buds

Zeina Jarikji[1,2,*], Lori Dawn Horb[1,2,*], Farhana Shariff[1], Craig A. Mandato[3], Ken W. Y. Cho[4] and Marko E. Horb[1,2,3,5,†]

During embryogenesis, the pancreas develops from separate dorsal and ventral buds, which fuse to form the mature pancreas. Little is known about the functional differences between these two buds or the relative contribution of cells derived from each region to the pancreas after fusion. To follow the fate of dorsal or ventral bud derived cells in the pancreas after fusion, we produced chimeric Elas-GFP transgenic/wild-type embryos in which either dorsal or ventral pancreatic bud cells expressed GFP. We found that ventral pancreatic cells migrate extensively into the dorsal pancreas after fusion, whereas the converse does not occur. Moreover, we found that annular pancreatic tissue is composed exclusively of ventral pancreas-derived cells. To identify ventral pancreas-specific genes that may play a role in pancreatic bud fusion, we isolated individual dorsal and ventral pancreatic buds, prior to fusion, from NF38/39 *Xenopus laevis* tadpoles and compared their gene expression profiles (NF refers to the specific stage of *Xenopus* development). As a result of this screen, we have identified several new ventral pancreas-specific genes, all of which are expressed in the same location within the ventral pancreas at the junction where the two ventral pancreatic buds fuse. Morpholino-mediated knockdown of one of these ventral-specific genes, *transmembrane 4 superfamily member 3* (*tm4sf3*), inhibited dorsal-ventral pancreatic bud fusion, as well as acinar cell differentiation. Conversely, overexpression of *tm4sf3* promoted development of annular pancreas. Our results are the first to define molecular and behavioral differences between the dorsal and ventral pancreas, and suggest an unexpected role for the ventral pancreas in pancreatic bud fusion.

KEY WORDS: *Xenopus*, Pancreatic bud, Tm4sf3, Tetraspanin, Annular pancreas

INTRODUCTION

The pancreas is a single endodermal organ that embryologically is derived from three distinct primordia: one dorsal and two ventral (Kelly and Melton, 2000; Kumar and Melton, 2003; Slack, 1995). The dorsal pancreatic bud arises first from the dorsal side of the duodenum immediately below the notochord, whereas the two paired ventral pancreatic buds develop slightly later adjacent to the hepatic diverticulum (Tremblay and Zaret, 2005). In mammals, the smaller left ventral bud usually regresses (Lammert et al., 2001; Lewis, 1911; Odgers, 1930), whereas in chick and *Xenopus* the two ventral buds will become part of the mature organ (Kelly and Melton, 2000; Kim et al., 1997). Each bud gives rise to different regions of the mature organ: the dorsal pancreas, which contributes to the body, neck and tail; and the ventral pancreas, which contributes to the head and uncinate process (Delmas, 1939; Uchida et al., 1999). In *Xenopus laevis*, the dorsal anlage is first apparent at NF35/36 at the level of the pronephros, whereas the two ventral buds develop slightly later at NF37/38 adjacent to the hepatic cavity, where it merges with the gastroduodenal cavity (Chalmers and Slack, 1998; Kelly and Melton, 2000; Pearl et al., 2009). [We refer to stages of *Xenopus* development as NF followed by the stage number as defined by Nieuwkoop and Faber (Nieuwkoop and Faber, 1967).] Following formation of these three separate buds, subsequent morphogenesis results, first, in the fusion of the two ventral buds by NF38/39 and, second, in the fusion of the dorsal and ventral buds at NF40.

Both endocrine and exocrine cells are found dispersed throughout the adult pancreas, but, in *Xenopus*, initial differentiation of these cell types occurs in a spatially and temporally distinct manner (Pearl et al., 2009). Endocrine cells are specified and arise initially only from the dorsal pancreas (Horb and Slack, 2002; Kelly and Melton, 2000). Beta cells are first specified prior to fusion of the dorsal and ventral pancreas at NF32, whereas alpha and delta cells are detected only in the pancreas from NF44/45. By contrast, acinar cell markers are first detected only in the ventral pancreas shortly after fusion at NF40, with expression spreading rapidly into the dorsal pancreas by NF44 (Horb and Slack, 2002). After NF46, however, endocrine and exocrine cells are present throughout the entire pancreas, with no dorsal-ventral differences. By contrast, in adult mammals dorsal-ventral differences are seen in the endocrine composition of islets. The dorsal islets contain normal shaped islets rich in insulin and glucagon cells, but few PP cells (Bencosme and Liepa, 1955; Suda et al., 1981; Wittingen and Frey, 1974). The exact opposite is seen in the head and uncinate process: the islets are irregular in shape, being rich in PP cells and poor in insulin and glucagon cells (Uchida et al., 1999; Yi et al., 2004).

Specification of the dorsal pancreas is not essential for normal development. In humans, dorsal pancreas agenesis has been reported as an uncommon congenital defect that, in most cases, is not diagnosed until the individual develops other symptoms later

[1]Laboratory of Molecular Organogenesis, Institut de Recherches Cliniques de Montréal, 110 Pine Avenue West, Montreal, QC H2W 1R7, Canada. [2]Montreal Diabetes Research Center, Centre de recherche du Centre Hospitalier de l'Université de Montréal, Montreal, QC H1W 4A4, Canada. [3]Department of Anatomy and Cell Biology and Division of Experimental Medicine, McGill University, Montreal, QC Canada. [4]Developmental Biology Center and the Department of Developmental and Cell Biology, University of California, Irvine, CA 92697-2300, USA. [5]Département de médecine, Université de Montréal, Montréal, QC H3T 3J7, Canada.

*These authors contributed equally to this work
†Author for correspondence (e-mail: marko.horb@ircm.qc.ca)

Accepted 31 March 2009

in life, such as diabetes mellitus or pancreatitis (Gilinsky et al., 1985; Guntz et al., 1976; Gurson et al., 1970; Klein et al., 1994; Lechner and Read, 1966; Shah et al., 1987; Wang et al., 1990; Wildling et al., 1993). On the other hand, there are no reports of ventral pancreas agenesis. Two congenital defects, however, have been attributed to improper development of the ventral pancreatic bud: pancreas divisum and annular pancreas (Cano et al., 2007). Pancreas divisum is a relatively common pancreatic congenital anomaly, with a prevalence of 5-10% (Agha and Williams, 1987). It occurs when the ventral and dorsal ducts do not fuse, resulting in the persistence of the dorsal accessory pancreatic duct (Klein and Affronti, 2004; Quest and Lombard, 2000). Annular pancreas, on the other hand, is a rare congenital defect that occurs when the ventral pancreas forms a complete ring around the duodenum, causing an obstruction of the duodenum (Jimenez et al., 2004; Ladd and Madura, 2001). Several hypotheses have been proposed to explain the development of annular pancreas (Baldwin, 1910; Kamisawa et al., 2001; Lecco, 1910). These hypotheses attribute the embryological origin of annular pancreas to defective ventral pancreas development, but this has not yet been proven. Although the genetic basis for this defect is not known, 42% of Indian hedgehog (Ihh) mutant mice developed annular pancreas (Hebrok et al., 2000). However, it is unclear how loss of Ihh contributes to the development of this condition.

To follow the fate of dorsal and ventral pancreatic bud-derived cells, we took advantage of the embryological benefits of *Xenopus* (Blitz et al., 2006; Pearl and Horb, 2008) and created chimeric transgenic Elas-GFP/wild-type embryos. We found that ventral pancreatic cells migrate extensively into the dorsal pancreas after fusion of the two buds during normal development, whereas the dorsal pancreas-derived cells do not. In addition, we also found that annular pancreatic tissue is populated exclusively by cells derived from the ventral pancreas. To uncover molecular genetic differences between the dorsal and ventral pancreatic buds that might explain the behavior of the ventral pancreatic bud, we isolated individual dorsal and ventral pancreatic buds prior to their fusion and compared their gene expression profiles using microarrays. As a result of this comparison, we identified several new dorsal and ventral-specific genes. Here, we present the functional analysis of one ventral specific gene, *transmembrane 4 superfamily member 3* (*tm4sf3*). Using antisense morpholino knockdown techniques, we examined its role in early pancreas development and found that it was involved in the regulation of pancreatic bud fusion and acinar cell development. By contrast, overexpression of *tm4sf3* was sufficient to promote development of annular pancreas. These results are the first to identify distinct behavioral and molecular differences between the dorsal and ventral pancreas.

MATERIALS AND METHODS

Embryological dissections

For the Elas-GFP transgenic/wild-type transplantation experiments, we fertilized eggs from *Xenopus* F2 Elas-GFP females with sperm from transgenic males, and simultaneously fertilized eggs from wild-type females with sperm from wild-type males. The embryos were grown at different temperatures overnight. Once the embryos reached NF19-20, we removed the vitelline envelopes and transplanted dorsal halves onto host embryos, from which we had removed an equivalently sized dorsal piece. The chimeric embryos were then placed in Noble agar to immobilize them, coverslips were placed on top of them to prevent the transplanted piece from moving and left to heal overnight. At NF44/45, we isolated whole guts from anesthetized tadpoles and photographed with the Leica DFC480 digital camera mounted onto a Leica MZ-16FA microscope. Individual liver/pancreas tissue samples were subsequently isolated from whole guts. The same method was followed to create chimeric embryos in which the entire endoderm was labeled, and to target *tm4sf3* overexpression or knockdown to dorsal or ventral endoderm.

Microarray analysis

Individual dorsal and ventral pancreatic buds were isolated at NF38-39 from numerous different fertilizations over the course of 3 months. Tissue samples were frozen until sufficient numbers were isolated and total RNA was then isolated using Trizol. Each pancreatic bud contained between 1 and 5 ng of total RNA, and we collected between 1000-3000 individual buds for each sample, two dorsal replicates and two ventral replicates. RNA analysis, cDNA preparation and hybridization to the Genechip Xenopus Genome Array were performed by the UCI DNA & Protein MicroArray Facility (University of California, Irvine), a shared resource, affiliated with the Chao Family Comprehensive Cancer Center, an NCI-designated Comprehensive Cancer Center (http://dmaf.biochem.uci.edu/).

The results were evaluated using the Affymetrix Expression Console and MAS5 algorithm. As we had only two replicates for each sample (too small a number to use methods based on analysis of variance or integral methods, such as RMA or PLIER), we employed the method of consecutive sampling and coincidence test (Guilbault et al., 2006; Novak et al., 2006a; Novak et al., 2006b; Novak et al., 2002). In two-array comparisons, the genes are ordered according to mean signal intensity and grouped in bins containing n consecutive genes (in the present case, n=25). The standard deviation is then calculated for each bin and the standard deviation function in linear approximation is determined by regression. Subsequently, specific probability intervals are evaluated so that the distance of corresponding points at upper and lower boundaries measured in standard deviations is invariant. The genes above and below a given interval are identified for both pairs of replicates and genes common to both sets are listed. Only those candidate genes above (ventral) or below (dorsal) 0.95 probability interval in three or all four comparisons are listed in Tables S1 and S2 in the supplementary material. The data discussed in this publication have been deposited in NCBI's Gene Expression Omnibus (Edgar et al., 2002), and are accessible through GEO Series accession number GSE13603 (http://www.ncbi.nlm.nih.gov/geo/query/acc.cgi?acc=GSE13603).

Plasmids, RT-PCR and whole-mount in situ hybridization

All clones were isolated by PCR from NF42 whole-gut cDNA, and confirmed by sequencing. For all constructs, primers were designed based on full-length sequence information obtained from GenBank, and the PCR products cloned into pCRII (Invitrogen). The GenBank Accession Number for *tm4sf3* is NM_001087390. RT-PCR was performed on isolated dorsal and ventral pancreatic buds and normalized to EF1-α. Whole-mount in situ hybridization with single probes were performed as described using BM Purple (Horb et al., 2003). Complete information for each clone is available upon request.

Antisense morpholino and mRNA injections

Antisense morpholino oligonucleotides were designed by Gene Tools. The antisense morpholinos were designed either to the translation start or in the 5′UTR. Morpholinos were injected into the dorsal vegetal blastomeres at the eight-cell stage. For functional analysis, we selected only those samples where the morpholino targeted the entire anterior part of the gut. Targeting to the stomach, liver and pancreas was confirmed by monitoring fluorescence from labeled oligonucleotides, only after isolation of whole guts from injected embryos. Those samples where only half the stomach or half the pancreas was targeted were not selected. The sequences of the antisense morpholinos used are: *tm4sf3* utr, 5′-ATGTGGGAAACG-AAGAGCTTCTTGA-3′; *tm4sf3* start, 5′-CACTTGCTAACCCCAG-CCATTTTGG-3′. For mRNA injections, *tm4sf3* was cloned into CS2+ and mRNA made using the Ambion mMessage machine kit. *tm4sf3* mRNA was injected along with *gfp* mRNA and targeting confirmed by examining fluorescence. Each of the mRNA and morpholino injection experiments was performed at least three times using different batches of embryos.

RESULTS

Ventral pancreas derived cells migrate extensively after fusion of the dorsal and ventral pancreas

To determine the spatial distribution of dorsal and ventral pancreatic bud cells in the pancreas after fusion, we monitored the fate of cells derived from each bud by selectively labeling either the dorsal or ventral pancreas. This was accomplished by producing chimeric wild-type/F2 Elas-GFP transgenic embryos in which either the dorsal or ventral pancreatic bud was derived from a transgenic donor embryo and thus GFP$^+$ (Jarikji et al., 2007). The Elas-GFP transgene directs expression throughout the entire pancreas at early tadpole stages (Beck and Slack, 1999). Hence, when the ventral pancreatic bud is derived from an Elas-GFP transgenic embryo, the ventral pancreatic cells would be GFP$^+$, whereas dorsal pancreatic cells would be unlabeled. After fusion has occurred, the fate of ventral pancreatic bud cells can be determined by examining the location of GFP$^+$ cells in the pancreas; the same can be done when the dorsal pancreatic bud is derived from an Elas-GFP transgenic embryo.

To produce these chimeric embryos, we transplanted part of the dorsal half of a wild-type or Elas-GFP transgenic NF20 embryo, which included the archenteron roof from where the dorsal pancreas is derived (Chalmers and Slack, 2000), onto the ventral half of a transgenic or wild-type host (Fig. 1A,H). At this stage, the dorsal and ventral endoderm is separated by the archenteron, thus defining the boundary between the dorsal and ventral endoderm, and allowing for consistent dissections. These chimeric embryos were named either $D_{tg}V_{wt}$ or $V_{tg}D_{wt}$ to indicate whether the dorsal (D) or ventral (V) half of the embryo was derived from a transgenic Elas-GFP embryo (tg) or a wild-type embryo (wt). The chimeras were then cultured until tadpole stage NF42-44 at which time we isolated the whole guts and examined the fate of GFP$^+$ cells in the pancreas.

When the ventral pancreas was derived from an Elas-GFP transgenic embryo ($V_{tg}D_{wt}$), we did not find a smooth transition between labeled and unlabeled cells in 70% of the recombinants (n=20) (Fig. 1B,C). Instead, ventral-derived GFP$^+$ cells were found intermingled with dorsal unlabeled cells in $V_{tg}D_{wt}$ chimeras (Fig. 1E,F). By contrast, when the dorsal pancreas was derived from an Elas-GFP transgenic embryo ($D_{tg}V_{wt}$), no dorsal GFP$^+$ cells were found within the ventral region of the pancreas in any of the recombinants (n=22) (Fig. 1I,J). Unlabeled ventral-derived cells, however, were found within the labeled dorsal pancreas in $D_{tg}V_{wt}$ chimeras (Fig. 1L,M). In both sets of chimeric embryos, ventral pancreas-derived cells were found within the dorsal pancreas, showing that ventral pancreas cells migrate more extensively than the dorsal pancreatic cells.

As the archenteron collapses after NF20 prior to gut formation, an alternative interpretation to our results is that ventral endoderm cells migrate into the dorsal pancreatic endoderm when the archenteron collapses, prior to pancreatic bud formation. Previous lineage tracing data in *Xenopus* showed that dorsal and ventral endoderm cells do intercalate within the intestine; however, they did not examine the relative fate of cells within the pancreas (Chalmers

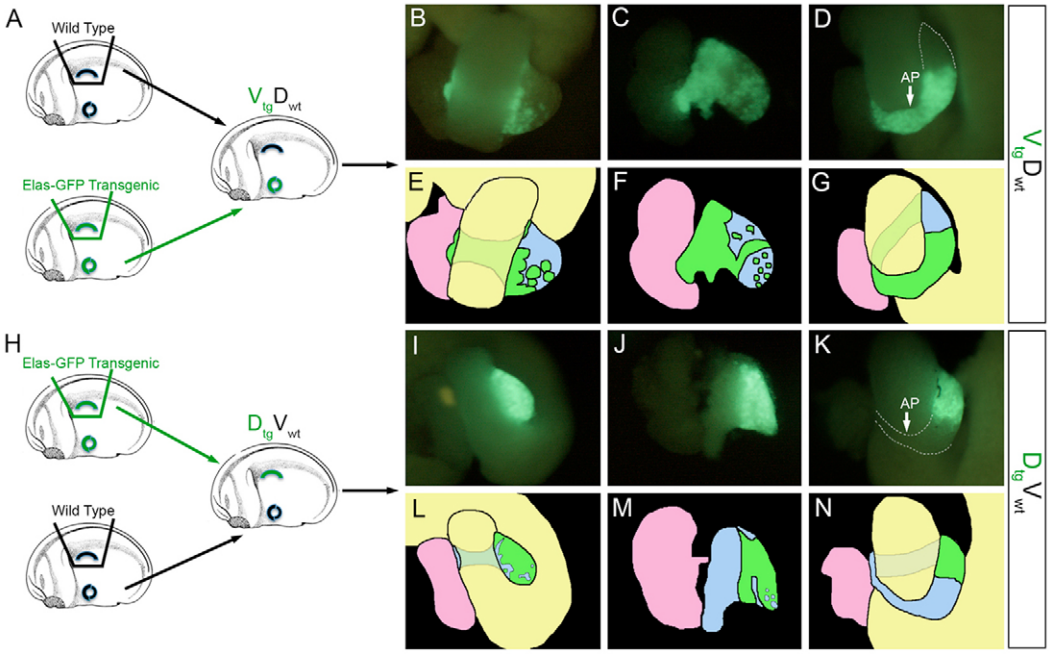

Fig. 1. Ventral pancreatic bud directs fusion of the dorsal and ventral pancreas. (**A**) Ventral halves of NF20 Elas-GFP transgenic embryos were recombined with dorsal halves of a wild-type embryo ($V_{tg}D_{wt}$) and grown to tadpole NF42. Only ventral pancreatic cells will be GFP$^+$. The prospective dorsal and ventral pancreatic buds are illustrated. (**B**) Fluorescent image of an isolated NF42 whole gut, revealing GFP$^+$ cells in the ventral pancreas, with punctate expression in the dorsal pancreas. (**C**) Isolated pancreas/liver tissue with no clear demarcation between the dorsal and ventral pancreas. Extensive GFP$^+$ cells are found throughout the dorsal region of the fused pancreas. (**D**) Annular pancreas (AP) phenotype that developed in a $V_{tg}D_{wt}$ recombinant. GFP$^+$ cells are found in the annular pancreas. (**E-G**) Color-coded drawings of the images in B-D. Green, GFP$^+$ transgenic pancreatic cells; blue, wild-type pancreatic cells; pink, liver; yellow, intestine. The region of the pancreas that lies behind the stomach is depicted using a lighter shade of green. (**H**) Schematic illustrating the recombination of dorsal wild-type and ventral transgenic halves ($D_{tg}V_{wt}$). Only dorsal pancreatic cells will be GFP$^+$. (**I**) Fluorescent image of an isolated NF42 whole gut showing the fate of GFP$^+$ dorsal pancreas cells. (**J**) Pancreas/liver tissue was isolated from the whole gut in order to better view the fate of GFP$^+$ cells in the pancreas. There is a sharp demarcation at the dorsal-ventral border; gaps of GFP$^-$ cells can be seen within the dorsal pancreas. (**K**) Annular pancreas that developed in a $D_{tg}V_{wt}$ recombination. No GFP$^+$ cells are found in the annular pancreas. (**L-N**) Color-coded drawings of the images in I-K.

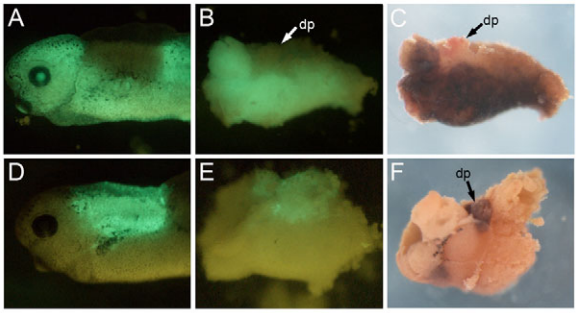

Fig. 2. Ventral endoderm cells do not mix with the prepancreatic dorsal endoderm after the archenteron closes. (**A**) Fluorescent image of a $V_{tg}D_{wt}$ chimeric embryo at NF32 showing GFP expression throughout the entire tadpole, but lacking in the dorsal region. (**B**) Isolated endoderm from NF35/36 $V_{tg}D_{wt}$ chimeric tadpole showing GFP fluorescence throughout the ventral endoderm, but lacking in the dorsal-most region of the endoderm. (**C**) Double in situ hybridization for ptf1a (red) and GFP (purple) of endoderm shown in B. No *gfp* mRNA is detectable in the ptf1a expression domain. (**D**) Fluorescent image of a $D_{tg}V_{wt}$ chimeric embryo at NF32 showing GFP expression only in the dorsal part of the tadpole. (**E**) Isolated endoderm from NF35/36 tadpole showing GFP fluorescence only in the dorsal layer of the endoderm. (**F**) In situ hybridization for ptf1a shown in G. The ptf1a expression domain is located in the dorsal layer of the endoderm. dp, dorsal pancreas.

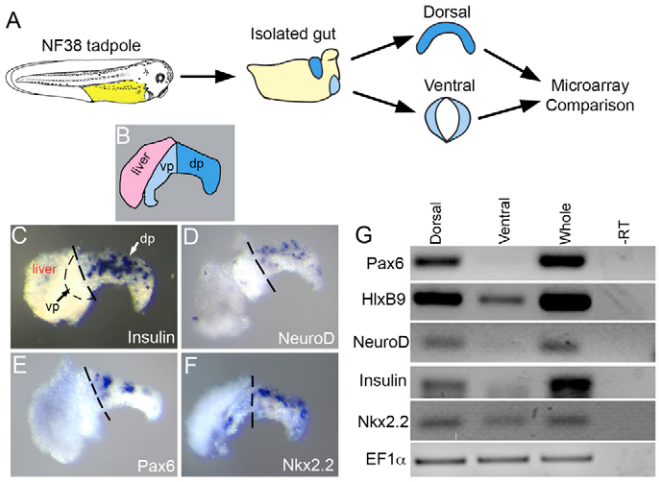

Fig. 3. Microarray analysis of dorsal and ventral pancreatic buds. (**A**) Schematic illustrating the experimental plan. Individual dorsal and ventral pancreatic buds were isolated from NF38 tadpoles. (**B**) Diagram of isolated liver and pancreas tissue samples, illustrating the distinct dorsal and ventral regions of the early pancreas, shortly after fusion. Dark blue, dorsal pancreas; light blue, ventral pancreas; pink, liver. (**C-F**) Whole-mount in situ hybridization on isolated liver/pancreas tissue at NF40 of selected pancreatic genes. dp, dorsal pancreas. (**G**) RT-PCR analysis of selected pancreatic genes in dorsal and ventral pancreatic bud samples used for the microarray.

and Slack, 2000). Therefore, to determine whether ventral endoderm cells migrated into the dorsal pancreatic endoderm during early tail bud stages when the archenteron collapses, we performed the same recombination experiments above, but instead of just labeling the pancreas the entire dorsal or ventral endoderm was labeled. We injected GFP mRNA into the vegetal pole of wild-type embryos, thus labeling the entire endoderm, and created chimeric embryos using GFP-injected and noninjected wild-type embryos (Fig. 2A,D). At NF35/36, we dissected out the entire endoderm and examined them for expression of *ptf1a* and *gfp* to determine whether ventral endoderm cells were present in the dorsal pancreatic bud. The dorsal-derived archenteron roof endoderm cells are a thin layer of cells and contribute only a small amount to the entire endoderm; they can be clearly seen when either the dorsal or ventral endoderm is labeled (Fig. 2B,E). When the ventral endoderm was labeled with GFP, we did not find any GFP^+ cells within the dorsal pancreatic bud, as marked by *ptf1a* expression (Fig. 2B,C; n=10). By contrast, when the dorsal endoderm was labeled, GFP expression co-localized with *ptf1a* expression (Fig. 2E,F; n=6). In agreement with these results, when we dissected pancreata from chimeric Elas-GFP/wt embryos at NF40 (immediately after fusion), we did not detect intermingling of GFP^+ and GFP^- cells (data not shown). In conclusion, these results agree with our Elas-GFP chimeric embryos showing that ventral pancreatic cells migrate into the dorsal pancreas only after fusion of the dorsal and ventral pancreatic buds has occurred.

In 10% of the Elas-GFP transgenic/wild-type chimeras (4/42) we also observed abnormal development of an annular pancreas (the rest of the gut developed normally). As only half of the pancreas was labeled, we were able to determine whether annular pancreas tissue was populated by ventral or dorsal-derived cells. When an annular pancreas developed in $V_{tg}D_{wt}$ recombinants, we found the entire annular pancreas to be GFP^+ (Fig. 1D,G). By contrast, in $D_{tg}V_{wt}$ recombinants, no GFP^+ cells were observed in the annular pancreas (Fig. 1K,N), demonstrating that annular pancreatic tissue is derived solely from ventral pancreatic cells. These results support the notion that cells derived from the ventral pancreatic bud migrate more extensively and suggest that genes localized to the ventral pancreatic bud may play primary roles in mediating migration and fusion of the pancreatic buds.

Isolation of dorsal and ventral pancreatic anlagen and their genetic differences

Based on the above results, we hypothesized that genes involved in regulating dorsal-ventral bud fusion and migration would be localized to the ventral pancreas. Therefore, to identify ventral pancreas-specific genes, we isolated dorsal and ventral pancreatic buds prior to their fusion at NF38/39 (2.5 days) and compared their gene expression profiles (Fig. 3A). In addition to the above data, our previous results also suggested that the ventral pancreas would be enriched with exocrine-specific genes, whereas the dorsal pancreatic bud would be enriched with endocrine-specific genes (Horb and Slack, 2002; Kelly and Melton, 2000). At early stages, just after fusion of the pancreatic buds, expression of several endocrine-specific markers (*neuroD*, *pax6* and *insulin*) was localized to the dorsal region of the pancreas (Fig. 3B-F). By contrast, we found that *Nkx2.2*, another endocrine transcription factor, was expressed in both dorsal and ventral regions of the pancreas (Fig. 3F). These known endocrine-specific genes provided us with positive controls for the dorsal pancreatic bud.

To determine whether our dissections of dorsal and ventral pancreatic buds were accurate, we examined whether differential expression of these endocrine-specific markers was evident in our isolated buds. In agreement with our whole-mount in situ data, we found *pax6*, *neuroD*, *insulin* and *hlxb9* to be enriched in the dorsal pancreatic bud, whereas *nkx2.2* was present in both dorsal and ventral pancreatic buds (Fig. 3G). These results confirmed that our embryological dissections were accurate and that molecular genetic

differences were faithfully maintained and detected in these isolated buds. We therefore used these samples to screen the *Xenopus* Affymetrix Genechip. Four different samples, two dorsal and two ventral, were reverse transcribed, labeled and hybridized to the *Xenopus* Affymetrix Genechip. Results were analyzed using the Affymetrix Expression Console and MAS5 algorithm, and because we only had two replicates, we employed the method of consecutive sampling and coincidence test (Guilbault et al., 2006; Novak et al., 2006a; Novak et al., 2006b; Novak et al., 2002). The results of this analysis yielded 158 genes as being ventral enriched and 68 genes as being dorsal enriched (see Tables S1 and S2 in the supplementary material).

In agreement with our hypothesis, the microarray data revealed dorsal enrichment of several endocrine differentiation markers [*insulin*, *prohormone convertase 2* (*pcsk2-A*), *secretogranin III* (*scg3-A*), *carboxypeptidase E* and *7B2 pituitary protein*] and pancreatic transcription factors (*neuroD*, *pax6* and *hlxb9)* (see Table S1 in the supplementary material). In fact, *insulin II*, *insulin I* and *pcsk2-A* were three of the most highly enriched dorsal genes, with 38-, 37- and 13-fold greater expression in the dorsal bud, respectively (see Table S1 in the supplementary material). As a first step to validate the microarray data, we examined the expression of several dorsal-enriched genes in isolated dorsal and ventral pancreatic buds by RT-PCR. We chose 12 of the most highly enriched genes (>2.5-fold) and found all to be highly enriched in the dorsal pancreas, which validates the microarray data (Fig. 4).

To define more accurately their localization within the pancreas, we examined the spatial expression of 12 dorsal-enriched genes at NF40 in isolated liver/pancreas tissue samples by whole-mount in situ hybridization. We did not use NF38/39 pancreatic buds (the stage when the buds were isolated for the microarray) because the individual pancreatic buds are much too small to process for whole-mount in situ analysis, and are very difficult to isolate in large numbers. NF40 is the earliest stage after fusion of the dorsal and ventral pancreatic buds when the tissue samples are easier to isolate, and still maintain their dorsal-ventral differences, as was seen for *insulin*, *neurod* and *pax6* (Fig. 3C-E). In addition to these three, we confirmed dorsal-specific localization for six other genes identified in the microarray: *hlxb9*, *pcsk2-A*, *scg3-A*, *frzb-1*, *brunol1* and *insm1* (Fig. 4C-E and data not shown). The expression pattern for eight of these genes was very similar, showing punctate domains of expression within the dorsal pancreas. Only *frzb-1* showed a different pattern of expression, being localized to the dorsal pancreatic mesoderm (data not shown). Overall, most of the top 20 dorsal-enriched genes are known endocrine-specific genes, whereas the majority of the remaining 48 genes are either unknown ESTs or are known genes that have not been studied in pancreas development.

Although many more genes were identified as enriched in the ventral pancreas (see Table S2 in the supplementary material), much less is known about the molecular genetics of ventral pancreas development. As with the dorsal subset, we initially selected a subset of genes with greater than twofold enrichment and confirmed their differential expression in isolated dorsal and ventral pancreatic buds by RT-PCR (Fig. 4B). Those selected were *transmembrane 4 superfamily 3* (*tm4sf3*), *transmembrane 4 superfamily member 4* (*tm4sf4*), *inter-alpha trypsin inhibitor heavy chain 2* (*itih2*), *ephrin B1*, *Ets2 repressor factor* (*erf*), *anterior gradient 2* (*agr2*) and *Xl.1424*. Ventral bud-specific expression was confirmed for five out of these seven genes – *tm4sf3*, *tm4sf4*, *itih2*, *agr2* and *Xl.1424* (Fig. 4B) – whereas *ephrin B1* and *erf* were equally expressed in the dorsal and ventral bud fractions.

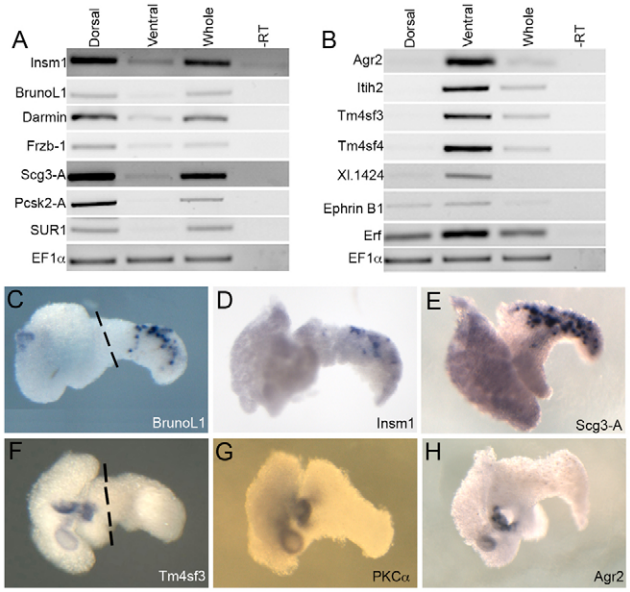

Fig. 4. Validation of microarray data. (**A**,**B**) Initial confirmation of the data by RT-PCR analysis of selected genes found to be enriched in either the dorsal or ventral bud fraction. (**C-E**) Dorsal-specific localization of *brunol1*, *insm1* and *secretogranin III* in isolated liver/pancreas tissue at NF40, except for *secretogranin III*, which is at NF44. Expression in all three instances is punctate. (**F-H**) Ventral pancreas-specific expression of *tm4sf3*, *pkc-alpha* and *agr2* at NF40/42. Expression is localized to a small region in the ventral pancreas, where the two ventral pancreatic buds fuse, and to where the bile duct emerges. Broken lines in C and F indicate the boundary of dorsal and ventral pancreas.

To define more precisely their spatial localization in the pancreas, we examined the expression pattern of several ventral genes in isolated liver/pancreatic tissue samples, and confirmed ventral pancreas-specific expression for *tm4sf3*, *pkc-alpha*, *agr2*, *slit2* and Xl.1424 (Fig. 4F-H; data not shown). All five were found to be expressed in the same region at the junction where the two ventral buds fuse. We did not detect expression of *ephrin B1* and *tm4sf4* in the pancreas, although abundant expression was detected in the liver, whereas *erf* and MGC83069 were expressed throughout the entire pancreas (data not shown). Unlike the dorsal bud fraction, the majority of genes identified in the microarray as ventral enriched were unknown and had not been characterized as being involved in pancreas development.

Tm4sf3 is required for acinar cell differentiation, dorsal-ventral pancreatic bud fusion and stomach development

One of the first ventral-enriched genes we chose to study was *transmembrane 4 superfamily member 3* (*tm4sf3*), which was enriched 10-fold in the ventral bud fraction. Tm4sf3 belongs to the tetraspanin family of proteins, which are cell-surface proteins that span the membrane four times, and are present in many different organisms (Hemler, 2005; Zoller, 2009). There are 33 vertebrate tetraspanins that are implicated in regulating cell migration and fusion, although their exact functions are not fully characterized (Berditchevski, 2001; Hemler, 2005; Lazo, 2007; Levy and Shoham, 2005a; Levy and Shoham, 2005b). *TM4SF3* was originally identified as the cDNA for the human tumor-associated antigen CO-029 (D6.1 in rat) expressed in gastric, colon rectal and pancreatic

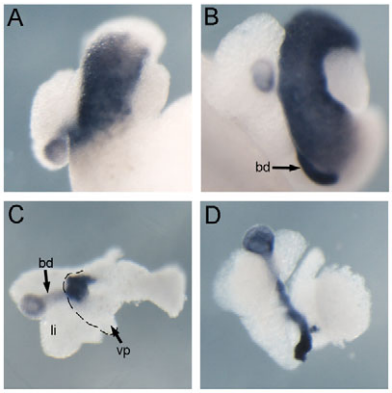

Fig. 5. Expression of *tm4sf3* in the gastrointestinal tract and pancreas. (**A**) NF40 whole gut showing localized expression of *tm4sf3* to the developing stomach and duodenum. (**B**) NF44 whole gut. *tm4sf3* expression persists in the stomach and duodenum, and is also now detected in the bile duct (bd). (**C**) Isolated pancreas/liver tissue at NF40, revealing expression of *tm4sf3* in the ventral pancreas (vp). Expression is localized to the junction where the two ventral pancreatic buds fused. A Small amount of expression is also evident in the bile duct. li, liver. (**D**) By NF44, ventral pancreas-specific expression decreased, but increased in the bile duct.

carcinomas (Szala et al., 1990). A previous microarray screen in mice identified *Tm4sf3* as being expressed in Pdx1-eGFP^{+} cells, although it was only expressed in the duodenum (Gu et al., 2004). The role of *tm4sf3* during embryonic development, however, has not been investigated.

To determine where *tm4sf3* was expressed in the whole embryo, we examined the developmental expression of *Xenopus tm4sf3* by whole-mount in situ hybridization. We did not detect expression of *tm4sf3* during gastrula, neurula or tail bud stages. Beginning at tadpole stage 40, *tm4sf3* expression was found throughout the stomach/duodenum (Fig. 5A), in agreement with the previous data in mice. As the gut continued to develop, expression of *tm4sf3* increased in the stomach/duodenum, and was also found enriched in the bile duct (Fig. 5B). As much of the pancreas is obscured by the stomach and duodenum at these stages, we examined its expression in the pancreas in isolated liver/pancreas samples. We found abundant expression of *tm4sf3* in the ventral pancreas at NF40, with low-level expression also in the bile duct (Fig. 5C). As mentioned above, the expression in the ventral pancreas was localized to the junction where the two ventral pancreatic buds fuse. By NF44 the expression of *tm4sf3* in the pancreas decreased, whereas its expression in the developing bile duct increased (Fig. 5D).

To address the function of *tm4sf3* in early pancreas development, we designed an antisense morpholino to the 5′UTR to inhibit its translation (see Materials and methods). As a control, we used a second morpholino designed to the translation start site of *tm4sf3* that did not affect translation. These *tm4sf3* morpholinos were injected at the eight-cell stage into the two dorsal vegetal blastomeres to target the anterior endoderm. Injection of 20 ng of the *tm4sf3*-utr morpholino resulted in a phenotype of a small ventral pancreas, a normal dorsal pancreas and liver; the stomach was also smaller and abnormal. The dorsal and ventral pancreatic buds had not fused and remained separate (Fig. 6). This phenotype was seen in 86% of injected tadpoles (n=197). Expression of *ptf1a* in the non-fused dorsal and ventral pancreatic buds was normal at NF41 (Fig. 6A,B). Expression of the liver marker *hex* was also normal, though in almost every case the liver was fused with the intestine (Fig. 6C,D). By contrast, we found reduced expression of the stomach/duodenum marker *frp5* (Fig. 6E,F). Targeting of the morpholino to only the dorsal pancreas did not affect fusion of the dorsal and ventral pancreatic buds (see below). Serial histological sections confirmed the lack of fusion between the dorsal and ventral pancreatic buds (Fig. 6Q-V). Three-dimensional reconstruction of the whole gut demonstrates clearly that, in contrast to control, the dorsal and ventral pancreatic buds remained separate (Fig. 6W,X).

To determine which pancreatic cell types were affected by loss of *tm4sf3*, we performed whole-mount in situ hybridization on whole guts for different pancreas markers. We were unable to detect expression of the late acinar differentiation marker *elastase* (Fig. 6I,J). As *tm4sf3* is not expressed in the dorsal pancreas, we were surprised to find that expression of *elastase* was inhibited in the unfused dorsal pancreatic bud. To rule out the possibility that loss of late acinar differentiation markers was due to nonspecific results from *tm4sf3* morpholino expression in the dorsal pancreatic bud, we specifically targeted knockdown of Tm4sf3 in the dorsal pancreas by creating chimeric *tm4sf3* morpholino/wild-type embryos. Dorsal halves of NF20 embryos injected with *tm4sf3* morpholino were transplanted onto ventral halves of wild-type embryos and grown to NF44, at which time we isolated the whole guts. Unlike the previous morpholino injection results (that were targeted to the entire anterior endoderm) fusion of the dorsal and ventral pancreatic buds and expression of *elastase* were normal (data not shown).

We next determined whether initial differentiation of exocrine pancreatic cells was normal in Tm4sf3 knockdown embryos by examining whether expression of the early exocrine differentiation marker, *pancreatic protein disulphide isomerase* (*XPDIp*), was affected by loss of *tm4sf3*. In contrast to *elastase*, we found normal expression of *XPDIp* in the unfused dorsal and pancreatic buds in *tm4sf3* morphants (Fig. 6K,L). We believe the reason for these differences in effects on exocrine differentiation markers is due to the fact that *XPDIp* is expressed in both dorsal and ventral pancreatic buds before they have fused at NF39, earlier than *elastase* (Afelik et al., 2004). It is possible that dorsal pancreas expression of late acinar differentiation markers is dependent on cell-cell interactions that initiate in the ventral pancreas, and knockdown of Tm4sf3 in the ventral pancreas disturbs this initial expression in the ventral pancreas.

In contrast to the effects on exocrine differentiation, we found normal expression of the endocrine marker *insulin* in the dorsal pancreas (Fig. 6M,N). However, in 45% of cases ectopic *insulin* expression was also detected in the ventral pancreatic bud (Fig. 6N). At this early stage, *insulin* expression is normally detected only in the dorsal pancreas, and is not expressed in the ventral part of the pancreas until NF45-46 (Horb and Slack, 2002). With regards to the other endocrine cell types, we found reduced expression of *somatostatin* and *glucagon* in the stomach and duodenum (Fig. 6M-P). Expression of these two endocrine markers is not detected in the pancreas until after NF44 (Pearl et al., 2009). In agreement with its spatial distribution, these results demonstrated that Tm4sf3 was necessary for pancreatic acinar cell differentiation and stomach/duodenal endocrine cell differentiation, but not for specification of endocrine beta cells. In addition to its affects on cell fate, we also found that knockdown of Tm4sf3 affected the proliferation of endodermal cells. In *tm4sf3* morphants, there was a 51% decrease in endodermal phospho histone H3 cells at NF40 (data not shown).

To confirm that the knockdown phenotype is directly related to the loss of Tm4sf3, we attempted to rescue the morpholino-induced phenotype by co-injecting *tm4sf3* mRNA lacking the 5′UTR along

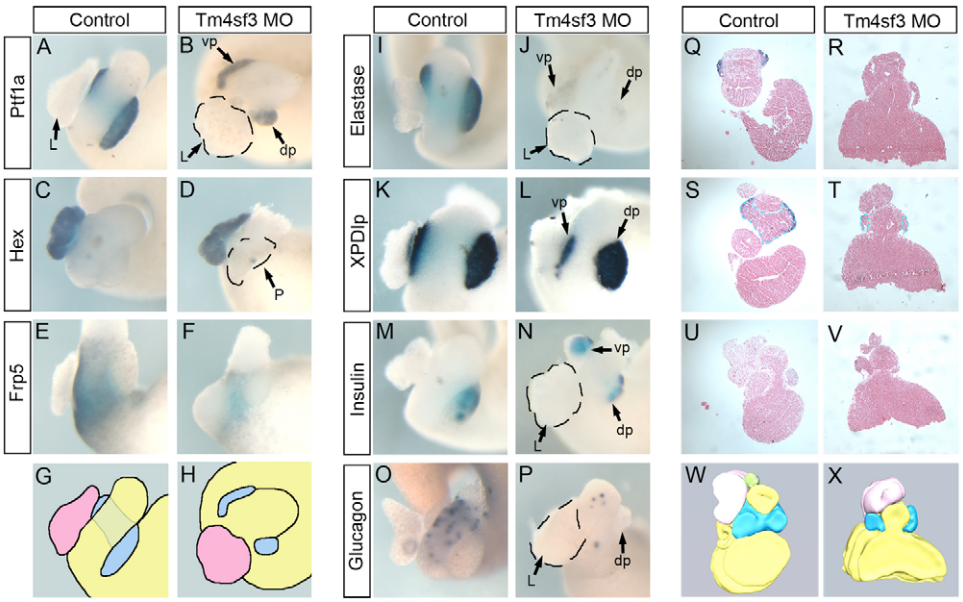

Fig. 6. Tm4sf3 is required for acinar and stomach/duodenum development. (**A**,**B**) Expression of the general pancreas marker Ptf1a is normal in *tm4sf3* morphants (*n*=7), but also reveals that the dorsal (dp) and ventral (vp) pancreatic buds have not fused. The liver position (L) has changed compared with normal and is present below the pancreatic buds in the region of the stomach/duodenum. (**C**,**D**) Expression of the liver marker Hex was normal (*n*=18). P, pancreas. (**E**,**F**) Expression of the stomach/duodenum marker frp5 was almost completely abolished (40/44). (**G**,**H**) Schematic highlighting the phenotype seen in Tm4sf3 knockdown embryos. The pancreas normally grows behind the duodenum, as illustrated by the darker shading in the wild-type gut. In *tm4sf3* morphants, the dorsal and ventral pancreatic buds do not fuse. (**I**,**J**) The acinar cell marker elastase was substantially reduced or completely abolished in Tm4sf3 knockdown embryos (19/27 absent, 8/27 reduced). (**K**,**L**) Expression of the early acinar differentiation marker XPDIp was normal in the dorsal and ventral pancreatic buds in *tm4sf3* morphants (*n*=42). (**M**,**N**) Insulin expression was normal in the dorsal pancreas in a little over half the cases (16/29). Interestingly, ectopic insulin expression was found in the ventral pancreatic bud in 45% of our samples (13/29). (**O**,**P**) No expression of glucagon or somatostatin was detected in the stomach/duodenum (*n*=8). At this stage, neither is yet expressed in the pancreas. (**Q-V**) Representative serial sections from an individual isolated NF42 whole gut that were previously stained for ptf1a expression. (**W**,**X**) Three-dimensional reconstruction of the samples based on all serial sections. Pancreas is blue, liver is pink, intestine is yellow and the gall bladder is green.

with 20 ng of the morpholino. At NF42, we examined the resultant tadpoles for morphological rescue of dorsal-ventral pancreatic bud fusion and acinar differentiation. In control embryos, the dorsal and ventral pancreatic buds have fused and elastase expression is detected throughout the entire pancreas (Fig. 7A). As previously demonstrated, the dorsal and ventral pancreatic buds did not fuse and no expression of elastase was detected in 84% (*n*=58) of *tm4sf3* morphants (Fig. 7B). When 1.8 ng of *tm4sf3* mRNA (lacking the 5′UTR) was co-injected with 20 ng of *tm4sf3* morpholino, expression of elastase was restored and the dorsal and ventral pancreatic buds fused in 53% of injected embryos (Fig. 7C, *n*=112). Forty-two percent of injected embryos still showed the knockdown phenotype, whereas 5% developed annular pancreas, indicative of an overexpression phenotype (see below). At mRNA doses greater than 1.8 ng, we observed less of a rescue to normal morphology and instead saw increased development of annular pancreas (data not shown). These results demonstrate that the morpholino-induced phenotype is specifically due to the loss of Tm4sf3.

Tm4sf3 promotes annular pancreas formation

We next examined whether *tm4sf3* was sufficient to promote ectopic migration and fusion of the dorsal and ventral pancreas by overexpressing *tm4sf3* mRNA. Following the same procedure as with the morpholino, *tm4sf3* mRNA was injected into the two dorsal vegetal blastomeres at the eight-cell stage. At doses lower than 1 ng, we did not observe any effects, whereas at 1.6 ng we observed a phenotype of annular pancreas in 79% of injected embryos (*n*=140). Within the ectopic pancreas, we detected abundant expression of acinar differentiation markers (Fig. 8A,B), but no endocrine marker expression (Fig. 8C,D). Development of other parts of the anterior endoderm was normal, and we did not observe any ectopic development of stomach or duodenal tissue (Fig. 8E,F). No change in expression of the early pancreas markers *ptf1a* and *pdx1* was observed at NF35 in *tm4sf3* injected tadpoles (data not shown). To determine whether the induction of annular pancreas by *tm4sf3* was due to increased proliferation, we stained injected embryos for phospho histone H3, but did not find any significant increase in proliferation within the annular pancreas (data not shown). Development of annular pancreas was confirmed in histological sections (Fig. 8C,F,I), and can be clearly seen in the three-dimensional reconstruction (Fig. 8L).

The fact that the only phenotype observed upon *tm4sf3* overexpression was development of annular pancreas suggested that *tm4sf3* overexpression was effective only in the ventral pancreas. To determine whether this was indeed the case, we targeted *tm4sf3* overexpression to the dorsal pancreas by creating chimeric *tm4sf3* mRNA/wild-type embryos. As outlined above with the *tm4sf3* morpholino, we transplanted dorsal halves of NF20 embryos overexpressing *tm4sf3* mRNA onto ventral halves of wild-type embryos. In these embryos, however, we did not observe development of annular pancreas (data not shown).

One of the ways in which tetraspanins have been shown to affect cell migration is by regulating integrin signaling through ligand-induced internalization (Berditchevski and Odintsova, 2007), and TM4SF3 has been shown to interact with integrins that affect cell motility and metastasis in colon, liver and pancreatic cancer cells (Claas et al., 1998; Claas et al., 2005; Gesierich et al., 2005; Herlevsen et al., 2003). The promotion of cell migration by another metastasis-associated tetraspanin, CD151, was found to be dependent on its ability to regulate integrin trafficking, as mutation of the C-terminal endocytosis/sorting motif in CD151 abolished its ability to promote cell migration (Liu et al., 2007). Similar tyrosine-based sorting motifs (YXXΦ) have been identified within the C terminus of 12 other tetraspanins, including TM4SF3 (Berditchevski

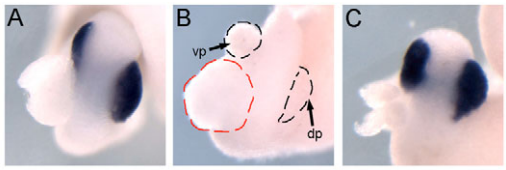

Fig. 7. *tm4sf3* mRNA rescues the morpholino knockdown phenotype. (**A**) Control whole gut stained for elastase expression. (**B**) Whole gut from embryo injected with 20 ng of morpholino. No elastase expression is detected, and the two buds did not fuse. Phenotype seen in 50/58 injected embryos. dp, dorsal pancreas; vp, ventral pancreas. The liver is outlined with a broken red line. (**C**) Whole gut from embryo co-injected with 20 ng *tm4sf3* morpholino and 1800 pg *tm4sf3* mRNA. Elastase expression is restored and the dorsal and ventral buds have fused. Rescue was seen in 59/112 injected embryos (53% rescue), 47/112 had the knockdown phenotype (42%) and 6/112 developed an annular pancreas (5%).

and Odintsova, 2007). To determine whether Tm4sf3 function is dependent on its interaction and internalization of integrins, we created a mutant Tm4sf3 without the last seven amino acids YCQIGKK (Tm4sf3Δc), and examined whether it was still able to promote formation of annular pancreas. We found that overexpression of *tm4sf3Δc* induced the development of annular pancreas (n=106, data not shown). However, the frequency with which *tm4sf3Δc* induced annular pancreas was slightly lower than that observed for *tm4sf3* injections carried out at the same time: 51% (54/106) when compared with 71% for *tm4sf3* (32/45). If integrin signaling were involved in *tm4sf3* promotion of ectopic migration and fusion of the pancreas, then we would not have expected to find development of annular pancreas in *tm4sf3Δc*-injected embryos. These results demonstrate that *tm4sf3* promotion of annular pancreas formation is not dependent on its interaction with integrins.

DISCUSSION

Little information exists pertaining to the functional relevance of the embryological origin of the pancreas from separate dorsal and ventral pancreatic buds. In this study, we demonstrate that ventral, and not dorsal, pancreatic bud cells migrate extensively after fusion. We also find that annular pancreatic tissue is populated exclusively by ventral pancreas derived cells. By comparing isolated dorsal and ventral pancreatic buds we have identified molecular genetic differences between them, and our identification of ventral pancreas specific genes is the first demonstration of such a subset of genes. Of these, we characterized the function of Tm4sf3 and defined a new role for it in pancreatic bud morphogenesis. This is the first study to examine differences between the dorsal and ventral pancreatic buds and demonstrate distinct functions for each bud.

By selectively labeling either the dorsal or ventral pancreas, we determined the fate of ventral and dorsal pancreatic bud cells in normal development and found that cells from the ventral pancreatic bud migrate extensively into the dorsal bud after fusion, whereas dorsal pancreatic bud cells do not. By recombining dorsal and ventral halves of transgenic F2 Elas-GFP embryos with wild-type embryos, we were able to selectively label either the dorsal or ventral pancreatic bud. When the dorsal pancreas was derived from transgenic embryos, we found a sharp boundary between unlabeled ventral pancreatic bud cells and GFP^+ dorsal pancreatic bud cells. By contrast, when the ventral pancreas was derived from Elas-GFP embryos, we found GFP expression throughout the dorsal pancreas

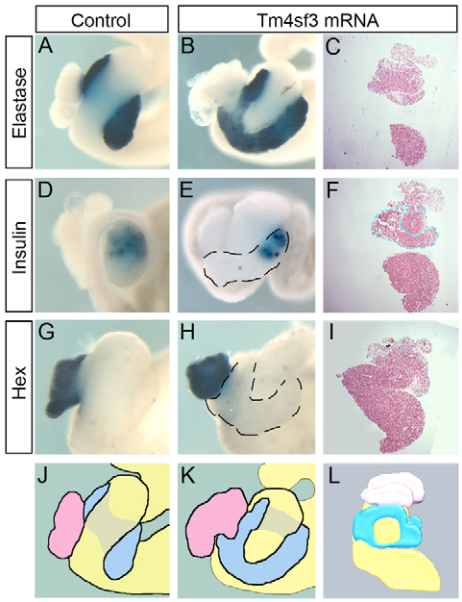

Fig. 8. Overexpression of *tm4sf3* mRNA resulted in annular pancreas development. (**A**,**B**) Expression of the acinar cell maker *elastase* is detected in the ectopic pancreatic tissue (n=19). (**D**,**E**) The endocrine marker *insulin* is not expressed (n=24). (**G**,**H**) Development of the liver was not affected by *tm4sf3* overexpression (n=17). The annular pancreas is outlined. (**J**,**K**) Schematic illustrating the development of annular pancreas. Pink, liver; blue, pancreas; yellow, GI tract. The pancreas normally grows behind the stomach, but in *tm4sf3*-injected embryos the pancreas also grows around the front of the duodenum. Lighter shading behind the yellow indicates the pancreas. (**C**,**F**,**I**) Representative serial sections from *tm4sf3*-injected whole gut. The pancreas encircles the stomach completely (blue outline in F). The stomach also appears slightly affected. (**L**) Three-dimensional reconstruction of histological sections illustrates the development of annular pancreas.

after fusion. These results are the first to directly examine the final spatial location of dorsal or ventral bud cells in the pancreas after fusion of the two buds.

One congenital disorder associated with inappropriate development of the ventral pancreas is annular pancreas, which occurs when the pancreas completely encircles the duodenum, causing a partial obstruction of the duodenum. Several different theories have been put forth to explain this developmental anomaly, including Baldwin's hypothesis and Lecco's theory (Baldwin, 1910; Cano et al., 2007; Kamisawa et al., 2001; Lecco, 1910). Although the accepted notion is that the annular pancreas is derived from ventral pancreatic bud cells, this has not been proven. In our chimeric embryos, we identified several different cases of annular pancreas, allowing us to lineage trace the fate of cells that populated the annular pancreas. Our results demonstrate that it is indeed ventral pancreatic cells that populate the annular pancreas. The fact that we find GFP^+ ventral pancreatic cells extending completely across the duodenum supports the notion that excessive migration of ventral pancreatic cells is responsible for the development of annular pancreas.

One the main phenotypes associated with the knockdown of Tm4sf3 was the lack of fusion of the dorsal and ventral pancreatic buds. Several reasons may explain this phenotype. The first explanation, which we favor, is that Tm4sf3 directly regulates the migration of ventral pancreatic bud cells. The fact that annular

pancreas develops in the gain-of-function phenotype supports this notion. An alternative explanation is that Tm4sf3 function is required only during fusion of the dorsal and ventral pancreatic buds, and not for migration. Although we cannot discount this possibility, we find it unlikely because if Tm4sf3 were simply involved in mediating fusion, then the buds should have migrated towards each other and simply not fused, but this is not what we observed. In conclusion, we believe that Tm4sf3 directly regulates the migration of ventral pancreatic bud cells.

Separate from the effects on pancreatic bud morphogenesis, the early appearance (stage 42) of endocrine β cells in the ventral pancreatic bud in *tm4sf3* morphants has interesting implications. In normal development, insulin is not expressed in the ventral region of the pancreas until NF45/46. This differentiation of β cells in the ventral pancreatic bud 3 days earlier in Tm4sf3 knockdown tadpoles suggests that Tm4sf3 may also have an unexpected role in the repression of endocrine cell differentiation. Identification of the molecular differences between the ventral pancreatic buds in Tm4sf3 knockdown and control tadpoles will help to identify genes that need to be repressed to allow differentiation of β cells in the ventral pancreas.

Our study is the first to define defective ventral pancreas development with normal liver and dorsal pancreas development. Previous results identified a bi-potential precursor population for the liver and pancreas (Deutsch et al., 2001), and two recent studies examining ventral pancreas development identified a relationship between liver and ventral pancreas development. In *Hex* and *Gata4* mutant mice, both liver and ventral pancreas specification is perturbed (Bort et al., 2004; Watt et al., 2007). However, the inhibition of ventral pancreas development is secondary to the liver defect. In vitro cultivation of prepancreatic ventral endoderm from $Hex^{-/-}$ mice was sufficient to restore pancreatic gene expression (Bort et al., 2004). In contrast to these studies, we found defective ventral pancreas development, but normal liver development in Tm4sf3 knockdown embryos.

This work was supported by grants from the Canadian Cancer Society (016243) and the National Institutes of Health (DK077197) to M.E.H. and from the NIH (GM075018) and the JDRF (VU31149R) to K.W.Y.C. Marko Horb is a junior 2 research scholar of the Fonds de la recherche en santé du Québec (FRSQ). Special thanks go to Dr Jaroslav P. Novak for his evaluation of the microarray data, Dr Esther Pearl for her drawings, Dr Tadayoshi Hayata for his help in the initial analysis of the data, Frédéric Bourque for his care of the frogs, Annie Vallée for the histological sections, and Dr Gregor Andelfinger and his laboratory for their help with the 3D reconstruction. Deposited in PMC for release after 12 months.

Supplementary material

Supplementary material available online at
http://dev.biologists.org/cgi/content/full/136/11/1791/DC1

References

Afelik, S., Chen, Y. and Pieler, T. (2004). Pancreatic protein disulfide isomerase (XPDIp) is an early marker for the exocrine lineage of the developing pancreas in Xenopus laevis embryos. *Gene Expr. Patterns* **4**, 71-76.
Agha, F. P. and Williams, K. D. (1987). Pancreas divisum: incidence, detection, and clinical significance. *Am. J. Gastroenterol.* **82**, 315-320.
Baldwin, W. M. (1910). A specimen of annular pancreas. *Anat. Rec.* **4**, 299-304.
Beck, C. W. and Slack, J. M. (1999). Gut specific expression using mammalian promoters in transgenic Xenopus laevis. *Mech. Dev.* **88**, 221-227.
Bencosme, S. A. and Liepa, E. (1955). Regional differences of the pancreatic islet. *Endocrinology* **57**, 588-593.
Berditchevski, F. (2001). Complexes of tetraspanins with integrins: more than meets the eye. *J. Cell Sci.* **114**, 4143-4151.
Berditchevski, F. and Odintsova, E. (2007). Tetraspanins as regulators of protein trafficking. *Traffic* **8**, 89-96.
Blitz, I. L., Andelfinger, G. and Horb, M. E. (2006). Germ layers to organs: using Xenopus to study 'later' development. *Semin. Cell Dev. Biol.* **17**, 133-145.
Bort, R., Martinez-Barbera, J. P., Beddington, R. S. and Zaret, K. S. (2004). Hex homeobox gene-dependent tissue positioning is required for organogenesis of the ventral pancreas. *Development* **131**, 797-806.
Cano, D. A., Hebrok, M. and Zenker, M. (2007). Pancreatic development and disease. *Gastroenterology* **132**, 745-762.
Chalmers, A. D. and Slack, J. M. (1998). Development of the gut in Xenopus laevis. *Dev. Dyn.* **212**, 509-521.
Chalmers, A. D. and Slack, J. M. (2000). The Xenopus tadpole gut: fate maps and morphogenetic movements. *Development* **127**, 381-392.
Claas, C., Seiter, S., Claas, A., Savelyeva, L., Schwab, M. and Zoller, M. (1998). Association between the rat homologue of CO-029, a metastasis-associated tetraspanin molecule and consumption coagulopathy. *J. Cell Biol.* **141**, 267-280.
Claas, C., Wahl, J., Orlicky, D. J., Karaduman, H., Schnolzer, M., Kempf, T. and Zoller, M. (2005). The tetraspanin D6.1A and its molecular partners on rat carcinoma cells. *Biochem. J.* **389**, 99-110.
Delmas, A. (1939). Les ébauches pancréatiques dorsales et ventrales. Leurs rapports dans la constitution du pancréas définitif. *Ann. Anat. Pathol.* **16**, 253-266.
Deutsch, G., Jung, J., Zheng, M., Lora, J. and Zaret, K. S. (2001). A bipotential precursor population for pancreas and liver within the embryonic endoderm. *Development* **128**, 871-881.
Edgar, R., Domrachev, M. and Lash, A. E. (2002). Gene Expression Omnibus: NCBI gene expression and hybridization array data repository. *Nucleic Acids Res.* **30**, 207-210.
Gesierich, S., Paret, C., Hildebrand, D., Weitz, J., Zgraggen, K., Schmitz-Winnenthal, F. H., Horejsi, V., Yoshie, O., Herlyn, D., Ashman, L. K. et al. (2005). Colocalization of the tetraspanins, CO-029 and CD151, with integrins in human pancreatic adenocarcinoma: impact on cell motility. *Clin. Cancer Res.* **11**, 2840-2852.
Gilinsky, N. H., Del Favero, G., Cotton, P. B. and Lees, W. R. (1985). Congenital short pancreas: a report of two cases. *Gut* **26**, 304-310.
Gu, G., Wells, J. M., Dombkowski, D., Preffer, F., Aronow, B. and Melton, D. A. (2004). Global expression analysis of gene regulatory pathways during endocrine pancreatic development. *Development* **131**, 165-179.
Guilbault, C., Novak, J. P., Martin, P., Boghdady, M. L., Saeed, Z., Guiot, M. C., Hudson, T. J. and Radzioch, D. (2006). Distinct pattern of lung gene expression in the Cftr-KO mice developing spontaneous lung disease compared with their littermate controls. *Physiol. Genomics* **25**, 179-193.
Guntz, M., Albaret, P., Joubaud, F. and Francois, H. (1976). Absence du corps et de la queue du pancréas et pancréatite chronique calcifiante. Pancréatectomie 'totale'. *Sem. Hop.* **52**, 1863-1867.
Gurson, C. T., Tahsinoglu, M., Yakacikli, S. and Ertugrul, T. (1970). A case of agenesis of the dorsal pancreas with interventricular septal defect in an infant. *Helv. Paediatr. Acta* **25**, 522-526.
Hebrok, M., Kim, S. K., St Jacques, B., McMahon, A. P. and Melton, D. A. (2000). Regulation of pancreas development by hedgehog signaling. *Development* **127**, 4905-4913.
Hemler, M. E. (2005). Tetraspanin functions and associated microdomains. *Nat. Rev. Mol. Cell Biol.* **6**, 801-811.
Herlevsen, M., Schmidt, D. S., Miyazaki, K. and Zoller, M. (2003). The association of the tetraspanin D6.1A with the alpha6beta4 integrin supports cell motility and liver metastasis formation. *J. Cell Sci.* **116**, 4373-4390.
Horb, M. E. and Slack, J. M. (2002). Expression of amylase and other pancreatic genes in Xenopus. *Mech. Dev.* **113**, 153-157.
Horb, M. E., Shen, C. N., Tosh, D. and Slack, J. M. (2003). Experimental conversion of liver to pancreas. *Curr. Biol.* **13**, 105-115.
Jarikji, Z. H., Vanamala, S., Beck, C. W., Wright, C. V., Leach, S. D. and Horb, M. E. (2007). Differential ability of Ptf1a and Ptf1a-VP16 to convert stomach, duodenum and liver to pancreas. *Dev. Biol.* **304**, 786-799.
Jimenez, J. C., Emil, S., Podnos, Y. and Nguyen, N. (2004). Annular pancreas in children: a recent decade's experience. *J. Pediatr. Surg.* **39**, 1654-1657.
Kamisawa, T., Yuyang, T., Egawa, N., Ishiwata, J. and Okamoto, A. (2001). A new embryologic hypothesis of annular pancreas. *Hepatogastroenterology* **48**, 277-278.
Kelly, O. G. and Melton, D. A. (2000). Development of the pancreas in Xenopus laevis. *Dev. Dyn.* **218**, 615-627.
Kim, S. K., Hebrok, M. and Melton, D. A. (1997). Pancreas development in the chick embryo. *Cold Spring Harb. Symp. Quant. Biol.* **62**, 377-383.
Klein, S. D. and Affronti, J. P. (2004). Pancreas divisum, an evidence-based review: part I, pathophysiology. *Gastrointest. Endosc.* **60**, 419-425.
Klein, W. A., Dabezies, M. A., Friedman, A. C., Caroline, D. F., Boden, G. H. and Cohen, S. (1994). Agenesis of dorsal pancreas in a patient with weight loss and diabetes mellitus. *Dig. Dis. Sci* **39**, 1708-1713.
Kumar, M. and Melton, D. (2003). Pancreas specification: a budding question. *Curr. Opin. Genet. Dev.* **13**, 401-407.
Ladd, A. P. and Madura, J. A. (2001). Congenital duodenal anomalies in the adult. *Arch. Surg.* **136**, 576-584.
Lammert, E., Cleaver, O. and Melton, D. (2001). Induction of pancreatic differentiation by signals from blood vessels. *Science* **294**, 564-567.

Lazo, P. A. (2007). Functional implications of tetraspanin proteins in cancer biology. *Cancer Sci.* **98**, 1666-1677.
Lecco, T. M. (1910). Zür morphologie des Pankreas annulare. *Sitzungsb. Akad. Wissensch.* **119**, 391-406.
Lechner, G. W. and Read, R. C. (1966). Agenesis of the dorsal pancreas in an adult diabetic presenting with duodenal ileus. *Ann. Surg.* **163**, 311-314.
Levy, S. and Shoham, T. (2005a). Protein-protein interactions in the tetraspanin web. *Physiology (Bethesda)* **20**, 218-224.
Levy, S. and Shoham, T. (2005b). The tetraspanin web modulates immune-signalling complexes. *Nat. Rev. Immunol.* **5**, 136-148.
Lewis, F. T. (1911). The bi-lobed form of the ventral pancreas in mammals. *Am. J. Anat.* **12**, 389-400.
Liu, L., He, B., Liu, W. M., Zhou, D., Cox, J. V. and Zhang, X. A. (2007). Tetraspanin CD151 promotes cell migration by regulating integrin trafficking. *J. Biol. Chem.* **282**, 31631-31642.
Nieuwkoop, P. D. and Faber, J. (1967). *Normal table of* Xenopus laevis *(Daudin)*, 2nd edn. Amsterdam, The Netherlands: North Holland
Novak, J. P., Sladek, R. and Hudson, T. J. (2002). Characterization of variability in large-scale gene expression data: implications for study design. *Genomics* **79**, 104-113.
Novak, J. P., Kim, S. Y., Xu, J., Modlich, O., Volsky, D. J., Honys, D., Slonczewski, J. L., Bell, D. A., Blattner, F. R., Blumwald, E. et al. (2006a). Generalization of DNA microarray dispersion properties: microarray equivalent of t-distribution. *Biol. Direct* **1**, 27.
Novak, J. P., Miller, M. C., 3rd. and Bell, D. A. (2006b). Variation in fiberoptic bead-based oligonucleotide microarrays: dispersion characteristics among hybridization and biological replicate samples. *Biol. Direct* **1**, 18.
Odgers, P. N. B. (1930). Some observations on the development of the ventral pancreas in man. *J. Anat.* **65**, 1-7.
Pearl, E. J. and Horb, M. E. (2008). Promoting ectopic pancreatic fates: pancreas development and future diabetes therapies. *Clin. Genet.* **74**, 316-324.
Pearl, E. J., Bilogan, C. K., Mukhi, S., Brown, D. D. and Horb, M. E. (2009). Xenopus pancreas development. *Dev. Dyn.* (in press).
Quest, L. and Lombard, M. (2000). Pancreas divisum: opinio divisa. *Gut* **47**, 317-319.
Shah, K. K., DeRidder, P. H., Schwab, R. E. and Alexander, T. J. (1987). CT diagnosis of dorsal pancreas agenesis. *J. Comput. Assist. Tomogr.* **11**, 170-171.
Slack, J. M. (1995). Developmental biology of the pancreas. *Development* **121**, 1569-1580.
Suda, K., Mizuguchi, K. and Hoshino, A. (1981). Differences of the ventral and dorsal anlagen of pancreas after fusion. *Acta Pathol. Jpn.* **31**, 583-589.
Szala, S., Kasai, Y., Steplewski, Z., Rodeck, U., Koprowski, H. and Linnenbach, A. J. (1990). Molecular cloning of cDNA for the human tumor-associated antigen CO-029 and identification of related transmembrane antigens. *Proc. Natl. Acad. Sci. USA* **87**, 6833-6837.
Tremblay, K. D. and Zaret, K. S. (2005). Distinct populations of endoderm cells converge to generate the embryonic liver bud and ventral foregut tissues. *Dev. Biol.* **280**, 87-99.
Uchida, T., Takada, T., Ammori, B. J., Suda, K. and Takahashi, T. (1999). Three-dimensional reconstruction of the ventral and dorsal pancreas: a new insight into anatomy and embryonic development. *J. Hepatobiliary Pancreat. Surg.* **6**, 176-180.
Wang, J. T., Lin, J. T., Chuang, C. N., Wang, S. M., Chuang, L. M., Chen, J. C., Huang, S. H., Chen, D. S. and Wang, T. H. (1990). Complete agenesis of the dorsal pancreas-a case report and review of the literature. *Pancreas* **5**, 493-497.
Watt, A. J., Zhao, R., Li, J. and Duncan, S. A. (2007). Development of the mammalian liver and ventral pancreas is dependent on GATA4. *BMC Dev. Biol.* **7**, 37.
Wildling, R., Schnedl, W. J., Reisinger, E. C., Schreiber, F., Lipp, R. W., Lederer, A. and Krejs, G. J. (1993). Agenesis of the dorsal pancreas in a woman with diabetes mellitus and in both of her sons. *Gastroenterology* **104**, 1182-1186.
Wittingen, J. and Frey, C. F. (1974). Islet concentration in the head, body, tail and uncinate process of the pancreas. *Ann. Surg.* **179**, 412-414.
Yi, S. Q., Akita, K., Ohta, T., Shimokawa, T., Tanaka, A., Ru, F., Nakatani, T., Isomura, G. and Tanaka, S. (2004). Cellular localization of endocrine cells in the adult pancreas of the house musk shrew, Suncus murinus: a comparative immunocytochemical study. *Gen. Comp. Endocrinol.* **136**, 162-170.
Zoller, M. (2009). Tetraspanins: push and pull in suppressing and promoting metastasis. *Nat. Rev. Cancer* **9**, 40-55.

Table S1. Dorsal enriched genes

Unigene ID	Gene title	Dorsal bud average	Ventral bud average	Fold enrichment in dorsal bud*
Xl.23623	Insulin II	1309.2	29.5	37.91
Xl.817	Insulin I	2320.0	57.5	37.12
Xl.1272	Prohormone convertase PC2	119.4	4.0	13.20
Xl.4241	Panza	532.7	40.2	11.78
Xl.6024	Glutamate carboxypeptidase-like protein 1	964.8	87.0	10.48
Xl.22766	MGC80496	46.6	1.6	7.11
Xl.647	Paired box gene 6 (Pax6)	33.9	1.1	5.52
Xl.15	Secretogranin III	31.3	1.1	5.17
Xl.23712	MGC84798	43.1	4.2	4.68
Xl.8836	Carboxypeptidase E	47.7	5.5	4.54
Xl.21888	Similar to complement component 6	97.0	19.5	3.97
Xl.8476	Carboxypeptidase E	71.2	16.5	3.30
Xl.1105	7B2 pituitary protein	21.6	1.6	3.29
Xl.330	Neurogenic differentiation 1 (NeuroD)	53.2	11.5	3.22
Xl.212	Frzb-1	164.0	47.0	3.16
Xl.932	Deoxyribonuclease I	507.5	159.9	3.08
Xl.1929	Frzb-1	66.1	18.0	2.87
Xl.6757	DEAH (Asp-Glu-Ala-His) box polypeptide 33	27.8	5.4	2.67
Xl.3378	Endod	503.4	184.3	2.66
Xl.647	Paired box gene 6 (Pax6)	21.3	3.1	2.64
Xl.14733	Insuloma-associated 1 (Insm1)	50.5	14.6	2.58
Xl.24557	MGC84299	17.3	1.8	2.56
Xl.25952	MGC68683	58.4	17.9	2.55
Xl.3011	Transcribed locus	209.2	77.0	2.55
Xl.13620	Transcribed locus	17.8	2.1	2.53
Xl.11047	Transcribed locus	95.0	32.8	2.51
Xl.15675	Similar to stromal cell derived factor receptor 2	266.7	101.9	2.50
Xl.17296	Transcribed locus	47.4	14.0	2.50
Xl.606	Collagen, type II, alpha 1	59.1	19.1	2.46
Xl.11165	Transcribed locus	51.3	16.0	2.45
Xl.637	Early growth response protein	69.8	23.6	2.44
Xl.5831	Similar to EH-domain containing 2	26.9	6.3	2.37
Xl.15742	Transcribed locus	25.7	5.8	2.37
Xl.10636	Transcribed locus	27.5	6.8	2.33
Xl.14367	Transcribed locus	139.6	56.3	2.28
Xl.6677	Cyclin E1	25.6	6.5	2.23
Xl.15089	Transcribed locus	364.3	158.6	2.23
Xl.6353	Glycine C-acetyltransferase (2-amino-3-ketobutyrate coenzyme A ligase)	342.8	151.0	2.20
Xl.647	Paired box gene 6 (Pax6)	18.3	3.4	2.17
Xl.12160	Trinucleotide repeat containing 4	23.0	5.6	2.16
Xl.198	Thrombospondin 3	49.1	17.8	2.15
Xl.24221	Transcribed locus	359.5	162.6	2.15
Xl.251	Dickkopf homolog 1	25.5	6.9	2.13
Xl.647	Paired box gene 6 (Pax6)	21.6	5.1	2.13
Xl.6690	LOC495431	58.3	22.4	2.13
Xl.12180	Putative growth hormone like protein-1	41.1	14.7	2.09
Xl.21515	C-fos proto-oncogene	19.5	4.5	2.05
Xl.15593	MGC82107	123.4	55.9	2.02
Xl.17442	Procollagen C-endopeptidase enhancer 2	31.2	10.5	2.01
Xl.26111	LOC100101272	11.4	0.7	2.01
Xl.24225	Transcribed locus	17.0	3.5	1.99
Xl.22355	Transcribed locus	246.5	119.2	1.99
Xl.684	Catenin arvcf-2ABC protein	38.4	14.8	1.94
Xl.24380	MGC68923	17.2	3.9	1.92
Xl.2466	MGC82199	166.1	81.4	1.92
Xl.986	Elav-type ribonucleoprotein (etr-1)	22.1	6.6	1.91
Xl.15089	Protocadherin PCNS	554.5	288.2	1.89
Xl.12488	Transcribed locus	12.2	1.5	1.88
Xl.23706	Transcribed locus	62.4	28.3	1.87
Xl.12129	Ftz-F1-related orphan receptor B	125.8	62.4	1.87
Xl.7523	Cdc25A	22.1	6.9	1.86
Xl.15089	Protocadherin PCNS	252.9	130.9	1.86
Xl.4042	MGC80644	20.9	6.2	1.86
Xl.24847	Transcribed locus	77.2	36.7	1.85
Xl.1040	Frizzled 10A	25.0	8.7	1.82
Xl.24545	Chromogranin A	25.9	9.6	1.78
Xl.11884	Cytoplasmic FMR1 interacting protein 2	18.5	5.4	1.77
Xl.14572	Transcribed locus	11.0	1.8	1.61

*Fold enrichment is adjusted to correct for unrealistically high ratios when denominator approaches zero. The ratio used to determine fold difference was VPB/(DPB+5).

Table S2. Ventral enriched genes

Unigene ID	Gene title	Dorsal bud average	Ventral bud average	Fold enrichment in ventral bud*
Xl.24589	Transmembrane 4 superfamily member 4	4.3	212.7	22.99
Xl.14821	LOC495168	56.3	959.6	15.65
Xl.24486	Transmembrane 4 superfamily member 3	2.8	82.7	10.62
Xl.5099	LOC495168	24.7	221.2	7.46
Xl.5040	Inter-alpha trypsin inhibitor, heavy chain 3	16.2	147.7	6.95
Xl.5040	Inter-alpha trypsin inhibitor, heavy chain 3	29.3	197.5	5.76
Xl.16348	MGC116540	7.3	69.4	5.65
Xl.866	Sonic hedgehog	3.2	46.3	5.62
Xl.3229	MGC86518	11.0	83.9	5.25
Xl.1122	Serum retinol binding protein	125.7	675.1	5.17
Xl.14976	Protein kinase C alpha	30.4	182.3	5.14
Xl.194	Lipocalin	6.1	56.3	5.09
Xl.11405	Calcium ATPase at 60A	28.8	171.9	5.09
Xl.534	Serotransferrin B	28.5	159.6	4.76
Xl.5569	LOC100049721	8.8	60.0	4.35
Xl.903	Alpha-1-antiproteinase	28.2	144.1	4.34
Xl.6263	Myosin light chain, phosphorylatable, fast skeletal muscle	35.3	174.6	4.34
Xl.424	Polysomal ribonuclease 1	34.3	168.1	4.28
Xl.14846	LOC100037012	5.3	43.0	4.19
Xl.1191	Connexin 30	36.5	173.6	4.18
Xl.1424	LOC100127277	100.5	426.4	4.04
Xl.13857	Transcribed locus	9.1	57.0	4.04
Xl.1464	Myosin, heavy polypeptide 4, skeletal muscle	13.0	72.4	4.03
Xl.18670	MGC115605	21.6	105.6	3.98
Xl.2151	Creatine kinase, mitochondrial 1 (ubiquitous)	66.3	277.0	3.89
Xl.1055	MGC53335	16.4	81.6	3.82
Xl.2200	Transcribed locus	72.0	288.1	3.74
Xl.1056	Myosin light chain, alkali, fast skeletal muscle	30.2	123.5	3.51
Xl.26470	Fibrinogen, A alpha polypeptide	74.7	277.8	3.48
Xl.6266	Embryonic epidermal lectin	185.2	657.9	3.46
Xl.2142	Fast troponin I	19.6	84.8	3.45
Xl.18975	LOC495296	12.2	58.6	3.40
Xl.9073	Transcribed locus	10.4	52.2	3.38
Xl.1055	MGC53335	16.8	71.7	3.29
Xl.280	Heparin cofactor II	29.7	113.5	3.27
Xl.5066	Protein C	13.5	60.2	3.26
Xl.9006	Myeloperoxidase, peroxidase 2'	49.5	176.8	3.25
Xl.1501	Transcribed locus	50.5	178.7	3.22
Xl.23713	Transcribed locus	115.3	386.5	3.21
Xl.1464	Myosin, heavy polypeptide 4, skeletal muscle	24.0	93.1	3.21
Xl.1642	Cytokeratin type II	62.4	215.9	3.20
Xl.14834	Transcribed locus	3.2	25.7	3.13
Xl.4801	Riboflavin-binding protein	72.2	241.3	3.12
Xl.5486	Similar to IgGFc-binding protein precursor (FcgammaBP)	68.7	229.9	3.12
Xl.2142	Fast troponin I	21.0	80.7	3.11
Xl.1501	Transcribed locus	135.8	432.3	3.07
Xl.12925	LOC495841	27.8	99.6	3.04
Xl.5482	MGC83069	382.2	1136.2	2.93
Xl.7895	MGC64421	75.6	235.7	2.93
Xl.25215	Similar to oncomodulin	4.8	28.0	2.86
Xl.5860	Creatine kinase, muscle	22.5	78.6	2.85
Xl.23949	LOC495173	21.6	74.9	2.82
Xl.23751	LOC495026	16.6	61.0	2.82
Xl.21150	MGC68589	37.8	120.5	2.81
Xl.578	GATA-5a	23.3	79.4	2.80
Xl.2142	Fast troponin I	23.3	78.3	2.77
Xl.3454	Similar to heterogeneous nuclear ribonucleoprotein H3 isoform a isoform 6	300.6	844.7	2.76
Xl.9653	Similar to Parvalbumin	18.4	64.3	2.74
Xl.879	Twist homolog 1	10.8	43.0	2.72
Xl.7590	XDCoH	36.7	113.0	2.71
Xl.10475	LOC495033	42.7	126.5	2.65
Xl.10642	Transcribed locus	2.5	19.6	2.61
Xl.26215	Alpha-1-microglobulin/bikunin precursor	457.6	1201.3	2.60
Xl.5846	MGC80184	6.7	30.0	2.57

Xl.5860	Creatine kinase, muscle	32.9	97.3	2.57
Xl.16704	MGC115198	75.1	203.8	2.55
Xl.6748	Glutamine fructose-6-phosphate transaminase 1	30.9	91.1	2.54
Xl.6005	CDNA clone 12F11	27.4	82.3	2.54
Xl.22590	Transcribed locus	47.8	133.4	2.53
Xl.5011	B fibrinopeptide	9.9	37.6	2.52
Xl.14940	Transcribed locus	38.2	108.6	2.52
Xl.14726	MGC53945	9.7	37.0	2.51
Xl.13814	Transcribed locus	4.7	24.3	2.50
Xl.5611	MGC80262	6.0	27.6	2.50
Xl.5846	Similar to actin alpha	13.4	45.0	2.44
Xl.24572	Fast skeletal troponin C alpha	15.1	48.7	2.42
Xl.5967	MGC80750	18.2	55.6	2.40
Xl.24530	Larval beta II globin	97.4	244.9	2.39
Xl.12727	LOC398669	11.0	38.2	2.39
Xl.23849	MGC85263	61.6	158.3	2.38
Xl.1642	Cytokeratin type II	160.3	390.3	2.36
Xl.888	Forkhead box A1	51.0	131.5	2.35
Xl.24267	Similar to plasminogen	30.4	82.8	2.34
Xl.302	Ephrin-B1	54.9	139.7	2.33
Xl.549	Putative alanine:glyoxylate aminotransferase	181.9	435.1	2.33
Xl.6256	MGC64326	15.0	45.7	2.29
Xl.6048	X-epilectin	20.8	59.0	2.29
Xl.14135	Similar to hydroxysteroid (17-beta) dehydrogenase 5	33.9	88.7	2.28
Xl.4788	MGC68535	3.3	19.0	2.28
Xl.1032	Fast skeletal troponin C beta	12.9	40.7	2.28
Xl.6171	Similar to protein kinase C and casein kinase substrate in neurons 3	15.1	45.6	2.27
Xl.13962	Transcribed locus	58.1	143.0	2.27
Xl.12750	LOC495373	3.9	20.1	2.26
Xl.25752	MGC115155	57.0	139.0	2.24
Xl.1685	Anterior gradient 2	8.5	30.3	2.24
Xl.2924	MGC53311	74.3	177.5	2.24
Xl.12563	Angiopoietin-like 2	7.3	27.5	2.23
Xl.526	Matrix metallopeptidase 9	14.7	43.5	2.21
Xl.5324	LOC398539	19.1	53.1	2.20
Xl.9800	LOC495178	12.4	38.1	2.19
Xl.21567	MGC69046	54.4	128.7	2.17
Xl.313	Similar to tropomyosin	12.7	38.4	2.17
Xl.1605	Envoplakin	12.4	37.6	2.16
Xl.9959	Degenerative spermatocyte homolog, lipid desaturase	14.8	42.5	2.15
Xl.1279	MGC80920	8.0	27.8	2.15
Xl.5021	Similar to complement component factor h	121.0	269.5	2.14
Xl.22702	Fumarylacetoacetate hydrolase	23.8	61.3	2.13
Xl.7213	Epid21	30.3	75.0	2.13
Xl.12414	Similar to poly (ADP-ribose) polymerase family, member 12	28.7	71.2	2.11
Xl.13506	Transcribed locus	18.2	49.0	2.11
Xl.5114	Transcribed locus	8.0	27.2	2.10
Xl.4591	Lactate dehydrogenase 2, B chain	106.1	231.8	2.09
Xl.19041	LOC398539	16.8	45.1	2.07
Xl.3362	Troponin T3, skeletal, fast	30.7	73.8	2.07
Xl.18233	MGC84148	125.9	267.8	2.05
Xl.10868	Galectin family xgalectin-VIa	14.7	40.2	2.04
Xl.1217	Hepatic nuclear factor 4	20.1	51.0	2.04
Xl.17370	Galectin family xgalectin-IVa	46.6	104.3	2.02
Xl.7590	XDCoH	117.7	246.5	2.01
Xl.1127	MGC64542	1528.6	3075.1	2.01
Xl.23949	LOC495173	41.9	94.1	2.00
Xl.6256	MGC64326	12.7	35.4	2.00
Xl.7590	XDCoH	114.1	237.2	1.99
Xl.5082	MGC68521	9.2	28.1	1.98
Xl.41820	Ets2 repressor factor (Erf)	9.6	29.0	1.98
Xl.20560	Transcribed locus	11.1	31.8	1.98
Xl.4128	LOC100037197	2.0	13.8	1.96
Xl.23954	Transcribed locus	13.3	35.9	1.96
Xl.10470	LOC100158309	6.0	21.5	1.96
Xl.41820	Ets2 repressor factor (Erf)	57.2	121.4	1.95

Xl.25047	Transcribed locus	8.6	26.5	1.95
Xl.16602	Transcribed locus	5.3	19.8	1.93
Xl.2503	MGC89895	60.3	126.1	1.93
Xl.13563	MGC80391	30.9	69.4	1.93
Xl.16754	MGC131044	28.9	65.3	1.93
Xl.11387	MGC82702	539.9	1045.9	1.92
Xl.6748	Glutamine fructose-6-phosphate transaminase 1	20.8	49.2	1.91
Xl.3881	Elongation of very long chain fatty acids (FEN1/Elo2, SUR4/Elo3, yeast)-like 1	243.0	470.0	1.90
Xl.10783	Kallikrein B, plasma (Fletcher factor) 1	1.8	12.8	1.89
Xl.26184	MGC64396	7.3	23.1	1.89
Xl.12772	Transcribed locus	67.9	137.2	1.88
Xl.25993	MGC84072	63.1	127.9	1.88
Xl.3153	Similar to oncomodulin	7.6	23.5	1.87
Xl.15894	Similar to periplakin	12.2	32.1	1.86
Xl.1126	MGC64611	1778.4	3324.5	1.86
Xl.1500	Villin	25.8	57.5	1.86
Xl.13909	LOC496348	33.4	70.8	1.85
Xl.289	Neuregulin 1	6.3	20.8	1.84
Xl.13260	Transcribed locus	112.3	213.4	1.82
Xl.3915	Transcribed locus	19.5	42.9	1.75
Xl.21934	FK506 binding protein 1B	20.9	45.2	1.75
Xl.5846	MGC80184	8.4	23.3	1.74
Xl.23810	Surfactant protein C	1.6	11.3	1.72
Xl.15841	LOC734942	7.8	22.0	1.72
Xl.5116	Transcribed locus	3.9	15.2	1.71
Xl.15870	Transcribed locus	3.1	13.6	1.69
Xl.15700	Similar to calsequestrin 2 (cardiac muscle)	1.3	10.6	1.68
Xl.21921	Similar to myozenin 1	2.5	12.2	1.63

*Fold enrichment is adjusted to correct for unrealistically high ratios when denominator approaches zero. The ratio used to determine fold difference was VPB/(DPB+5).